Design and Fabrication of a Fabry-Pérot Cavity Antenna for the $\mathrm{K_u}$-band

Pablo Mateos-Ruiz, Alberto Hernández-Escobar, Elena Abdo-Sánchez, Carlos Camacho-Peñalosa
{pablomr, ahe, elenaabdo, ccp}@ic.uma.es
Dpto. de Ingeniería de Comunicaciones, Universidad de Málaga – Andalucía Tech,
E.T.S. de Ingeniería de Telecomunicación, Bulevar Louis Pasteur 35, 29010 Málaga, Spain.

***Abstract*—A design of a directive antenna based on a Fabry-Pérot cavity is described, using a single metallic partially reflecting surface (PRS) in front of a coaxial-fed patch antenna. The main features of this type of antennas are their low profile and single feeding point. The design is initially carried out following an approximate ray model analysis using the extracted PRS characteristics from electromagnetic simulations. The antenna performance is also simulated, obtaining a directivity of $20.6\,\mathrm{dBi}$ for $15.25\,\mathrm{GHz}$, and verifying its predicted behaviour. Furthermore, a prototype is manufactured at the group premises and some measurements are presented.**

I. Introduction

Fabry-Pérot Cavity Antennas (FPCAs) have gained popularity over the last few years as a compact low-cost solution for designing very directive antennas in the microwave and millimetre-wave regions. FPCAs have a single feeding point, decreasing their complexity compared to feeding networks used in conventional array antennas. This solution was first proposed by G. V. Trentini in [1], and it has been further studied to this day. This technique is based on the operating principle of Fabry-Pérot resonators, using a passive partially reflecting surface in front of a ground plane. Thereby, a leaky-wave and beamforming effect is introduced, which increases the directivity of the primary source inside the resulting cavity.

The antenna bandwidth and the frequency for which the main resonance occurs strongly depend on the characteristics of the PRS and its separation from the ground plane. Therefore, the PRS design is crucial. In this case, its partial reflection is obtained from a frequency selective surface (FSS) made of apertures on a conducting plane. FSSs are arrays of elements commonly used for filtering electromagnetic waves which are partially reflecting near their resonance frequency. Moreover, they are planar structures easy to model and manufacture, making them convenient for building a prototype.

In this paper, an analytical and numerical study on the design process of this type of FPCA is presented. The simple ray theory from [1] has been used for obtaining the main design expressions and theoretical radiation patterns. It is based on multiple reflections between the ground plane and the PRS, which are both assumed to be infinite. In practice, however, the finite size of the antenna must be taken into account to achieve a high gain and good efficiency. Besides, the radiation pattern will be affected by the diffracted fields at the antenna edges. All these effects are accounted for through electromagnetic simulations using Ansys® HFSS software.

This antenna is designed to operate in the $\mathrm{K_u}$-band (12–18 GHz), mainly used in satellite communications. The purpose is to study the directivity that can be achieved with this type of technique and its limitations. Also, a prototype of this antenna has been manufactured at our premises at the University of Málaga with low-cost materials, which is also shown along with the explanation of the fabrication process taken and some preliminary measurements.

II. Simplified Ray Model Analysis

Being the first analysis model derived for FPCAs in [1], it is the simplest one while providing key information for the design of these antennas. A brief outline of the ray model analysis is made below.

The structure is composed of a radiation source on a conducting plane and a PRS at a distance D parallel to it. These surfaces are assumed to be infinite, thus the electromagnetic field originated at the source will bounce between both surfaces until completely transmitted through the PRS. The source generates an electric field

$$\boldsymbol{E_{source}}(\theta) = \boldsymbol{E_0} f(\theta)$$

and the PRS is assumed to be lossless, homogeneous, isotropic and characterized by its reflection coefficient $R = r\,e^{j\phi}$, dependent on frequency and the angle of incidence θ.

As derived in [1], each ray transmitted through the PRS will have a complex amplitude $\boldsymbol{A_n}$, being its sub-index the number of times it has bounced between the PRS and the ground plane. Knowing the expression of the first transmitted ray

$$\boldsymbol{A_0} = \boldsymbol{E_0} f(\theta)\sqrt{1-R^2}\,e^{-jk\frac{D}{\cos\theta}},$$

where k is the wavenumber, the amplitude of any ray at the same wavefront as a function of it can be expressed as

$$\boldsymbol{A_n} = \boldsymbol{A_0}\big(-R\,e^{-jk2D\cos\theta}\big)^n$$

and the total electric field would be the sum of all these partial rays, being its intensity in the far-field

$$\boldsymbol{E_T}(\omega,\theta) = \sum_{n=0}^{\infty} \boldsymbol{A_n} = \boldsymbol{E_0} f(\theta)\frac{\sqrt{1-R^2}\,e^{-jk\frac{D}{\cos\theta}}}{1+R\,e^{-jk2D\cos\theta}}. \quad (1)$$

Consequently, the relation between the cavity radiated power and the source delivered power, called *Transmissivity*, can be obtained as

$$\frac{|\boldsymbol{E_T}(\omega,\theta)|^2}{|\boldsymbol{E_0}|^2} = \frac{(1-r^2)\,f^2(\theta)}{1+2r\cos\left(\phi+\pi-\frac{4\pi}{\lambda}D\cos\theta\right)+r^2}. \quad (2)$$

Note that the transmissivity and the antenna directivity are not the same, although they are related by a scale factor depending on the radiation pattern for each frequency. Maximum

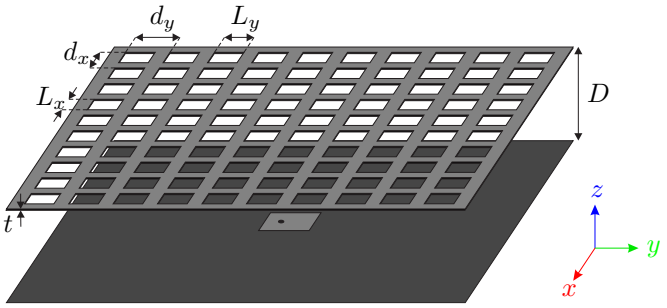

Fig. 1. Cavity with the selected PRS design.

power at broadside direction ($\theta = 0°$) is obtained when

$$\phi + \pi - \frac{4\pi}{\lambda} D = 0 \tag{3}$$

and hence, the resonance distance D_r between the PRS and the ground plane can be derived as follows

$$D_r = \left(\frac{\phi}{\pi} + 1\right)\frac{\lambda_r}{4} + N\frac{\lambda_r}{2}, \qquad N \in \mathbb{Z} \tag{4}$$

where λ_r is the desired cavity resonance wavelength. Additionally, the maximum transmissivity for the resonance distance can be obtained through the following expression [2]

$$\frac{|\boldsymbol{E_T}(\omega, 0°)|^2}{|\boldsymbol{E_{source}}(\omega, 0°)|^2} = \frac{1 - r^2}{(1 - r)^2} = \frac{1 + r}{1 - r} \tag{5}$$

and making (2) to equal half of its maximum, an expression for the half-power fractional bandwidth is attained

$$\text{FBW} = \frac{\Delta\lambda_{-3dB}}{\lambda_r} = \frac{2}{\phi + \pi}\text{acos}\left[1 - \frac{1}{2}\frac{(1 - r)^2}{r}\right]. \tag{6}$$

From these expressions, the usual resonant structure behaviour can be analysed. The more reflective the PRS is, the greater the maximum transmissivity the cavity can offer at the expense of narrower bandwidth.

III. Design of the FPCA

The design process of a simple FPCA with a resonance frequency of around 15 GHz is explained. First, the design of the PRS must be decided and, then, its reflection coefficient characterized in order to choose the exact parameters of the PRS for the desired maximum transmissivity. The radiation source must be designed as well, taking into account that it needs to be planar and easy to feed.

A. PRS

Following some initial design decisions in [3], the PRS is composed of a simple metallic sheet of thickness $t = 300\,\mu\text{m}$ and a matrix of square apertures in it (slots) with a periodicity of $d_x = d_y = 5.8\,\text{mm}$ (0.29λ at 15 GHz), as shown in Fig. 1. The periodicity is smaller than the wavelength, which is necessary for the PRS to be considered homogeneous. The size of the apertures sides $L = L_x = L_y$ is obtained from the reflection coefficient value through electromagnetic simulations.

Assuming a desired maximum transmissivity of around 18 dB, from (5) a reflection magnitude of $r = 0.97$ is obtained. Through electromagnetic simulations in HFSS using periodic boundary conditions and Floquet ports, the S-parameters of an infinitely long PRS can be calculated from

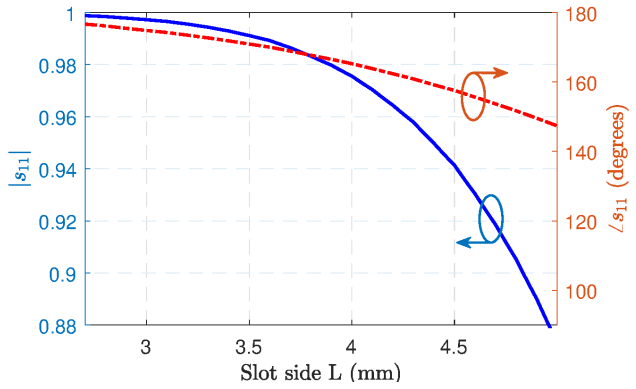

Fig. 2. PRS reflection for normal incidence as a function of the slot side size obtained from electromagnetic simulations.

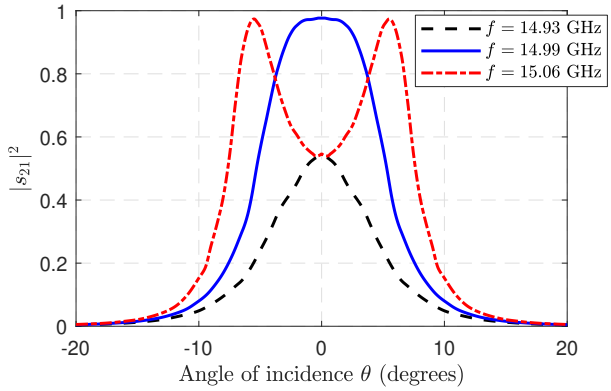

Fig. 3. PRS transmission characteristics as a function of the incidence angle for different frequencies obtained from electromagnetic simulations.

a single periodic cell. As a matter of fact, the unit cell is simulated with rounded corners of radius 1 mm to account for the size of the drill used in the manufacturing stage, as will be explained in Section V. A parametric analysis is performed under plane wave normal incidence condition and electric field linearly polarised in x-direction (which is equivalent to y-direction due to the PRS symmetry). The magnitude and phase of the reflection coefficient for different side sizes L and $f = 15\,\text{GHz}$ are shown in Fig. 2.

From these results, it can be extracted that for $L = 4.1\,\text{mm}$ the PRS has $s_{11} = 0.9704\,e^{j163.82°}$ and, from (4), $D_r = 9.55\,\text{mm}$ is achieved for this particular configuration. Furthermore, it is also verified that the PRS characteristics do not change rapidly neither in frequency nor for angles close to normal incidence.

In addition, an approximation of the cavity transmission characteristics can be accomplished through a *Defect Cavity Model* usually used to analyse more complex partially reflecting structures [4] [5], which is based on the resonance principle of Fabry-Pérot. This way, simulating by periodic boundary conditions two parallel unit cells separated a distance $2D_r$, the results in Fig. 3 are obtained. It can be observed that the maximum transmission for normal incidence occurs at $f = 14.99\,\text{GHz}$ with a half-power beamwidth of $\Delta\theta = 10.7°$, giving an approximate geometrical directivity of around 25.5 dBi. It is also noticed the usual FPCA frequency-dependent patterns [3]: for lower frequencies than the resonance one, the transmission decreases, while for greater

frequencies, a beam split behaviour is produced. Finally, a transmission bandwidth of 0.97% is obtained, which correlates with the theoretical value of $FBW = 1\%$ (6) for the achieved PRS reflection.

B. Radiation source

A rectangular patch antenna is selected as the radiation source because of its convenience, simple analysis, low profile, and easy feeding through a coaxial cable from below the ground plane. In order to ensure the analytical model assumption that the cavity is filled with air, the dielectric of the patch antenna is supposed to be air too. Due to the materials available, the substrate thickness is $h = 2\,\mathrm{mm}$ and so, the width (x-axis) and length (y-axis) of the patch to resonate at $15\,\mathrm{GHz}$ will be $W = 9.1\,\mathrm{mm}$ and $L = 8.9\,\mathrm{mm}$, respectively [6].

The feeding point of the patch is off-centered along the y-axis (Fig. 1). Therefore, the electric field will be mainly linearly polarized in the YZ plane. To find the exact feeding-point position, electromagnetic simulations are carried out including a typical $50\,\Omega$ coaxial connector into the model. Thereby, it is found that feeding the patch a distance $d = 3.8\,\mathrm{mm}$ from the center, a return loss above $30\,\mathrm{dB}$ is achieved for $15\,\mathrm{GHz}$ with an antenna gain of $8.7\,\mathrm{dBi}$.

IV. Simulations

First, the finite size of the antenna needs to be accounted for. The amount of field transmitted through the PRS is proportional to the size of the antenna, the rest being scattered at the edges. This way, a smaller antenna will have bigger sidelobes at the expense of lower directivity. Conversely, if the antenna is too big, the directivity will be more similar to the theoretical case, but almost no field will reach the edges of the PRS, decreasing the antenna efficiency. Due to computational limitations, a PRS size of 20x20 slots ($11.6\mathrm{x}11.6\,\mathrm{cm}^2$) is selected.

A simulation of the whole antenna (Fig. 1) is carried out in HFSS with the previously designed parameters and a frequency sweep around the resonance. Fig. 4 shows the antenna gain for both the FPCA and the patch antenna without the PRS, in order to compare the increase in directivity between them. These patterns are obtained for $f = 15.2\,\mathrm{GHz}$, obtaining a FPCA gain of $20.6\,\mathrm{dBi}$, an increase of $11.8\,\mathrm{dB}$ respect to the gain of the patch. The sidelobe level remains below $-11\,\mathrm{dB}$ with respect to the main lobe level for the E-plane and below $-13\,\mathrm{dB}$ for the H-plane. However, the sidelobe level increases for higher frequencies (beam split effect related) while decreasing for lower ones. Cross-polarization levels are below $-30\,\mathrm{dB}$ in both planes.

The frequency of these radiation patterns is the one for which the FPCA achieves maximum gain, as can be noticed in Fig. 5. In addition, a theoretical estimation for the broadside gain is computed from the designed PRS reflection and radiation patterns obtained from (2). A qualitative agreement is verified between the simple ray theory and simulations, with a slightly higher resonance frequency ($f = 15.25\,\mathrm{GHz}$) than the one predicted, giving a 1.6% relative error. This is caused by analytical model assumptions that are not satisfied in practice, such as the infinite PRS size or the plane wave incidence condition. In any case, the resonance frequency can be easily corrected slightly changing the distance between both sheets. Furthermore, the maximum gain is some decibels below the theoretical asymptotic value due to the sidelobes produced by diffracted fields at the antenna edges and the patch antenna performance inside the cavity.

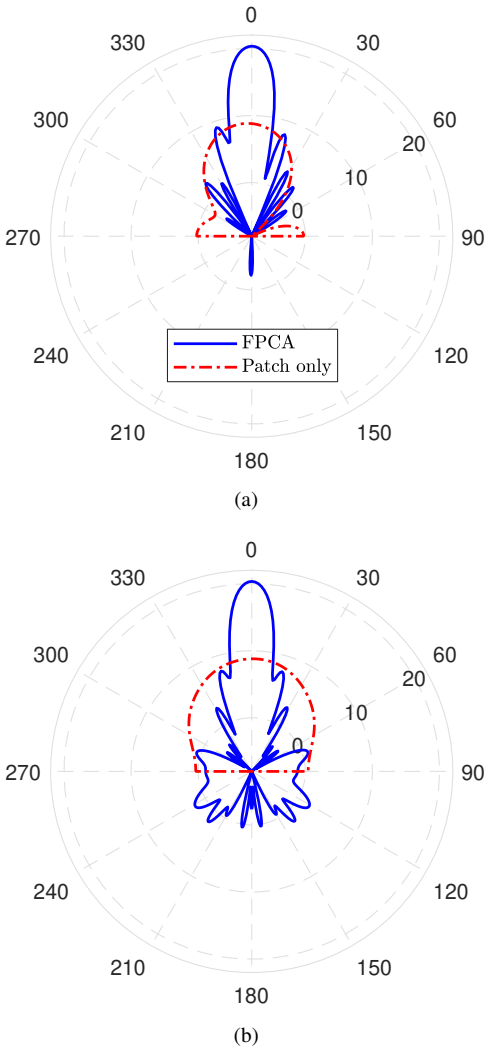

Fig. 4. Simulated gain comparison between designed FPCA and patch-only antenna for $f = 15.2\,\mathrm{GHz}$ in (a) the E-plane and (b) the H-plane.

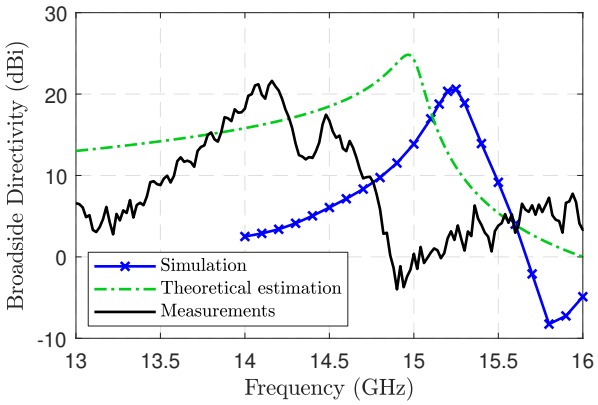

Fig. 5. FPCA gain in broadside direction as a function of frequency.

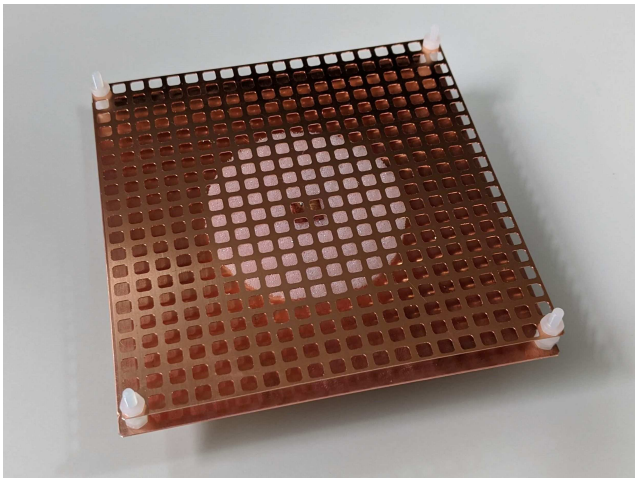

Fig. 6. Antenna Prototype.

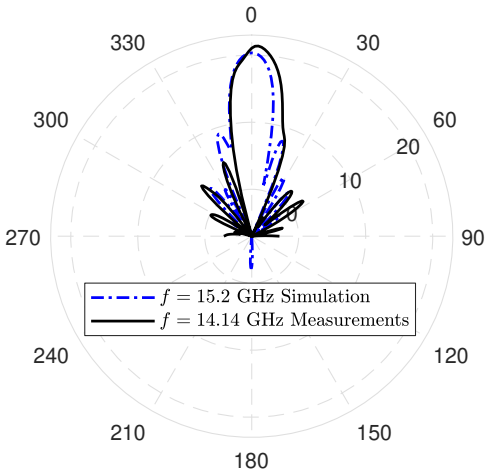

Fig. 7. Gain comparison between FPCA measurements and simulations for their resonance frequencies in the E-plane.

V. Fabrication

A prototype of the antenna is built to verify the previous work, explaining the manufacturing process below. Clearly, some design parameters have been chosen depending on the available materials. Both the ground plane and the PRS are copper sheets of $11.6\,\mathrm{cm}$ side (around 6λ side at $15\,\mathrm{GHz}$). As the cavity must be filled with air, the spacing between these two sheets is achieved through some nylon screws and nuts in the corners holding them separated a fixed distance. The PRS slots, the screw holes and the ground plane feeding point are drilled using a LPKF ProtoMat S103 PCB milling machine. As aforementioned said, the drill used had a radius of $1\,\mathrm{mm}$, thus the PRS was designed considering it.

The patch antenna is built using a Eccostock SH foam with $\epsilon_r \approx 1$ and $2\,\mathrm{mm}$ thickness as dielectric, mainly to support the patch on it. As this material is not metallized, a copper tape of width $9.1\,\mathrm{mm}$ is used for making the patch. A $50\,\Omega$ SMA coaxial connector with $4.1\,\mathrm{mm}$ outer diameter and Teflon insulation is soldered to the ground plane and the patch, sticking it to the foam. Before placing the PRS over it, its reflection coefficient is measured, accomplishing a good return loss value around $14\,\mathrm{GHz}$.

The whole antenna is assembled with four nuts on each screw between the sheets and another one to keep the PRS still, resulting in the structure shown in Fig. 6. Some measurements have been carried out at the group premises with a network analyzer proving that the prototype works qualitatively. The resonance frequency attained for this structure is around $14.1\,\mathrm{GHz}$ with a directivity of around $21\,\mathrm{dBi}$ (Figs. 5, 7). The observed frequency shift is due to both the limited precision at adjusting the resonance distance in practice and the attempt to align the resonances of the patch and the FPCA.

VI. Conclusions

Following a simple ray theory approach, the design of a Fabry-Pérot cavity antenna consisting of a slotted metallic PRS and a primary patch antenna has been carried out. The analytical and numerical study has been presented, finding good agreement between theoretical and simulated results. It is relevant that the ray model is a theoretical method which, despite its simplicity, gives an easy way to design FPCAs with a very acceptable outcome. The antenna has been simulated obtaining a directivity of almost $21\,\mathrm{dBi}$. With regard to increasing the directivity and the bandwidth further, aperiodic PRSs or multiple layer structures would be required.

In addition, a prototype has been built and has served to illustrate the relatively easy and inexpensive process of its fabrication. Also, qualitative agreement has been found between measurements and simulations. For future work, the use of a metallized-substrate patch should be considered for the radiating element in order to decrease manufacturing tolerances. Although the use of a dielectric inside the cavity has not been contemplated in the ray model, it can be easily introduced by characterizing the reflection of the dielectric-on-top-of-ground-plane structure.

Acknowledgements

The development of this research project is being possible thanks to the Initiation to Research Grant of the *I Plan Propio de Investigación y Transferencia* of the Universidad de Málaga. This project has also received funding from the Spanish *MCIU/AEI/FEDER (Programa Estatal de I+D+i Orientada a los Retos de la Sociedad)* under grant RTI2018-097098-J-I00.

References

[1] G. V. Trentini, "Partially reflecting sheet arrays," *IRE Transactions on Antennas and Propagation*, vol. 4, no. 4, pp. 666–671, October 1956.

[2] Z. Liu, "Effect of primary source location on fabry-perot resonator antenna," in *2009 Asia Pacific Microwave Conference*, Dec 2009, pp. 1809–1812.

[3] N. Guerin, S. Enoch, G. Tayeb, P. Sabouroux, P. Vincent, and H. Legay, "A metallic fabry-perot directive antenna," *IEEE Transactions on Antennas and Propagation*, vol. 54, no. 1, pp. 220–224, Jan 2006.

[4] M. T. Xu, L. Si, H. X. Jiang, and X. Lv, "An x-band high-gain low-profile dipole antenna based on electromagnetic band-gap," in *2018 International Conference on Microwave and Millimeter Wave Technology (ICMMT)*, May 2018, pp. 1–3.

[5] C. Cheype, C. Serier, M. Thevenot, T. Monediere, A. Reineix, and B. Jecko, "An electromagnetic bandgap resonator antenna," *IEEE Transactions on Antennas and Propagation*, vol. 50, no. 9, pp. 1285–1290, Sep. 2002.

[6] C. A. Balanis, *Antenna Theory: Analysis and Design*. Wiley-Interscience, 2005.